IFSCC 2025 full paper (IFSCC2025-973)

"Revolutionary Sunscreen Technology: Broad-Spectrum (UV + Blue Light) Protection with Non-Penetrating Filters, Pollution Protection, Translucent Jelly Texture and Customizable Shades, and Skin Tone Correction"

Weixiong Huang[1,2], Hongjuan Kuang[1,2], Xueping Chen[1], Wenwen Zhang[1,2], Kai Na Hung[1,2,*]

[1] Ausmetics Daily Chemicals (Guangzhou) Co. Ltd. No.1 Jinxiu Rd, Guangzhou Economic & Technical Development District, China.

[2] Glowgenix BioTech Ltd. Room 1109, 11/F, Austin Tower, 22-26 Austin Ave, Tsim Sha Tsui, KLN, Hong Kong SAR, China.

1. Introduction

Topical sunscreen application is recognized as one of the most effective strategies for preventing sun-induced skin damage [1]. Despite significant advancements in the efficacy and cosmetic appeal of sunscreens in recent years, a primary challenge remains ensuring human safety by preventing skin penetration [2-3]. Clinical studies have shown that sunscreens can permeate the skin and enter systemic circulation [3-5], potentially leading to adverse effects, particularly estrogenic effects [6-7]. This underscores the urgent need for effective and safe UV absorbers and formulation technologies that minimize skin penetration [1, 4]. Additionally, there is a growing market demand for broad-spectrum protection against both UV and blue light.

In this study, we introduce a novel sunscreen formulation technology that integrates advanced encapsulation techniques with multifunctional benefits. The formulation employs a water-in-oil system using silicone oil to encapsulate UV absorbers, complemented by an oil-in-water system containing active ingredients such as astaxanthin and rutin. These active compounds are microencapsulated into particles ranging from 200 to 500 nm using a water-based solution containing PPG-13-decyl-tetradeceth-24 and polyquaternium-61. The two systems are seamlessly combined to form a translucent oil-in-water-in-oil structure, designed to provide and optimize wide-spectrum light protection, pollution protection, skin tone correction, and sensory experience. The characteristics of the formulated representative sunscreens are analyzed through multiple experiments.

2. Materials and Methods

2.1 Experiment samples

Sunscreen: a sunscreen was formulated by microencapsulated UV absorbers using silicone oil to form a water-in-oil system.

Astaxanthin sunscreen: besides the water-in-oil system containing UV absorbers, an oil-in-water system containing 1% astaxanthin emulsified with PPG-13-decyltetradeceth-24 and polyquaternium-61 was developed. The two systems are seamlessly combined to form a translucent oil-in-water-in-oil sunscreen. The ingredient of the sunscreen contained: WATER, GLYCERIN, POLYDIMETHYLSILOXANE, BENZYL BENZIMIDAZOLE SULFONIC ACID, BENZYL BENZIMIDAZOLE TETRASULFONATE DISODIUM, P-PHENYLENEDIAMINE BIS(2-NAPHTHYLSULFONYL), ETHYL HYDROXYETHYLCELLULOSE, GLYCEROL ETHYL ETHER-26, SODIUM HYDROXIDE, POLYSILOXANE-15, PANTHENOL, POLYDIMETHYLSILOXANE PEG-10/15 CROSSPOLYMER, PHENOXYETHANOL, POLYDIMETHYLSILOXANE ALCOHOL, PEG-10 POLYDIMETHYLSILOXANE, WHALE WAX BASE PEG/PPG-10/1 POLYDIMETHYLSILOXANE, ETHYL HEXYL GLYCERIN, ASTAXANTHIN, BUTYLENE GLYCOL, DIPROPYLENE GLYCOL, PPG-13-MYRISTYL TETRADECYL ETHER-24, SODIUM CITRATE, POLYQUATERNIUM-61, TOCOPHEROL (VITAMIN E), and TETRAHYDROXYL-4-(BIS(BUTYLHYDROXY)HYDROCINNAMATE) ESTER.

Rutin sunscreen: similar to astaxanthin sunscreen, except the active ingredient was 0.5% rutin instead of astaxanthin.

Guaiazulene sunscreen: similar to astaxanthin sunscreen, except the active ingredient was 2% guaiazulene instead of astaxanthin.

Astaxanthin and guaiazulene sunscreen: similar to astaxanthin sunscreen, except the active ingredients were astaxanthin and guaiazulene mixture.

2.2 Characterization of Astaxanthin Sunscreen

The physical properties of astaxanthin sunscreen were examined using a polarizing microscope (PZ620TC-20MBI3, AmScope, USA). Particle size distribution of the astaxanthin sunscreen was determined using a laser diffraction particle size analyzer (Bettersize 3000 Plus, Bettersize, China). The analyzer was set to automatic mode with a reflection rate of 1.52, absorption rate of 0.1, and a reflection rate of 1.333, employing the Mie optical model, focus position, and measurement angle. Samples were dissolved in water, sonicated for 5 min, rotated at 202 rpm, and measured in triplicate to ensure reproducibility.

2.3 Human Patch Test

Following the HRIPT method outlined in Chapter 2 of the China Safety Technical Specifications for Cosmetics (2015 Edition) [8], the test involved 30 volunteers (4 male and 26 female), aged 21 to 38 years (average age 27.3 ± 4.8 years) who met the inclusion criteria. A sample of 0.020 - 0.025 g was applied to a 50-mm² area on the forearm (one sample per forearm) for 24 h. After 24 h, the samples were removed, and the skin response was evaluated at 0.5, 24, and 48 h post-treatment. The skin response was recorded according to the specified method..

2.4 *In vitro* SPF Value Test

SPF and PFA measurements were conducted following the Q/GDFX02-2023 Cosmetic In Vitro Sun Protection SPF Value Measurement Methods. Samples were uniformly applied onto 3M

Transpore tape (3M, Transpore™, US) at 2 mg/cm², kept in the dark for 15-25 min, and measured using SPF-290AS automated SPF analyzer (Solar Light Comp, Inc., US) by scanning from 290 nm to 400 nm. Each sample was measured in triplicate.

2.5 *In vivo* SPF and PFA Value Test

The test was performed following the sun protection test SPF and PFA determination methods as described in Chapter 8 of the China Safety Technical Specifications for Cosmetics (2015 Edition) [8].

2.5.1 SPF Determination

For SPF determination, 10 volunteers (4 males and 6 females), aged 21 to 55 years (average age 36.4 ± 11.9 years), who met the inclusion criteria, participated in the test. A reference sample with SPF of 16.1 ± 2.4 was included. Before testing, the minimum erythema dose (MED) value of the subjects' skin to 290 – 400 nm UV radiation was determined by exposing five points on their backs to varying dosages of UV radiation. The lowest dosage that caused red spots 24 h post-radiation was considered the MED. On the day of testing, a sample of (2.00 ± 0.05) mg/cm² was applied to five spots on the back. The irradiation dosages were selected according to the standard requirements and were carried out under four conditions: 1) Normal skin. 2) Skin coated with a reference substance (prepared according to the high SPF standard). 3) Skin coated with the innovative sunscreen. 4) Skin coated with the general sunscreen. After 24 h, the MED for the four conditions were recorded, and SPF was calculated as the MED value of protected skin divided by the MED value of unprotected skin.

2.5.2 PFA Determination

For PFA determination, 10 volunteers (6 males and 4 females), aged 19 to 43 years (average age 31.1 ± 7.6 years), who met the inclusion criteria, participated in the test. The test procedures were similar to SPF testing. A reference sample with SPF of 4.4 ± 0.6 was included. Before the test, the minimum persistent pigment darkening (MPPD) value of the subjects' skin to 320 – 400 nm UV radiation was determined and recorded at the end of the test. PFA was calculated as the MPPD value of protected skin divided by the MPD value of unprotected skin.

2.5 Skin Penetration Evaluation Through *In Vivo* Raman Spectroscopy

The Raman spectroscopy test was performed in accordance with the GB/T 40219-2021 General Specification for Raman Spectrometer [9]. A volunteer's forearm test area was cleaned and acclimated to a controlled environment at (22 ± 2) °C and (50 ± 10)% humidity for 30 min. The sample was applied at a concentration of 5 mg/cm² to a 1 × 1 cm² skin area for 30 min, after which it was washed off. At 0 and 6 h post-application, Raman spectra were collected from two points within the test area in parallel. Each point was measured five times using a point-by-point mapping approach in an x-z coordinate system, with a 5 μm depth difference and a 20 × 120 μm scanning area. The measurements were conducted using the LabRAM Odyssey (HORIBA) spectrometer at a laser power of 2.68 mW and an integration time of 0.5 s. The Raman spectra of the sample were also measured for reference. The Raman

spectroscopy data were analyzed using Labspec (HORIBA) software, and statistical analysis was performed using ORIGIN 2017.

2.6 Anti-pollution Test

An *in vivo* test was conducted to evaluate whether the sunscreen can protect skin from pollution. A volunteer's hands were cleaned and acclimated to a controlled environment at (22 ± 2) °C and (50 ± 10)% humidity for 30 min. A uniform layer of 0.05 g of sunscreen was applied to the back of the left hand and allowed to form a film for 15 min, while the back of the right hand served as a negative control. Subsequently, an equal amount of carbon powder, filtered through a 200-mesh sieve (to mimic PM2.5 pollution), was brushed onto the backs of both hands and left, and gently pat the back of the hand to simulate the friction from daily activities. After 10 min, the backs of both hands were then washed with running water at 25°C for 10 s, gently rubbed in a circular motion with fingertips three times, dried using paper towels, and imaged. The test was repeated three times to ensure consistency.

2.7 Skin Stickiness Test

An *in vivo* test was conducted to evaluate the stickiness of sunscreen after application to the skin. Similar to the anti-pollution test, a subject's hands were washed and dried, and a uniform layer of 0.05 g of sunscreen was applied to the back of the left hand and allowed to form a film for 15 min, while the back of the right hand served as a negative control. Both hands were then submerged with the backs facing downward into a pool of 2–5 mm foam balls for 5 s, slowly removed, and held in the air for 10 s. The number of foam balls adhering to the back of each hand was then counted. The test was repeated three times, with fresh foam balls used for each repetition.

2.8 Statistical Analysis

Data analysis was conducted using GraphPad Prism software. Results were expressed as mean ± SD. Comparisons between groups were performed using two-tailed t-tests and Wilcoxon signed-rank tests, with $p < 0.05$ considered a significant difference..

3. Results

3.1 Characterization of Sunscreens

3.1.1 Physical Appears of Sunscreens

Our formulation strategy involved the integration of a water-in-oil system with an oil-in-water system to create a translucent oil-in-water-in-oil structure. By incorporating various colored ingredients into the oil-in-water phase, we successfully developed a range of sunscreen gels exhibiting a spectrum of uniform colors (Figure 1). This means the innovative approach not only enhances the aesthetic appeal of the sunscreens but also ensures the uniformity of color distribution across the product line.

Figure 1. Visual characteristics of sunscreens. 1) – 4) showcase sunscreens infused with various colored water-soluble plant extracts. Panel 5 presents a sunscreen formulation containing guaiazulene, a compound known for its blue-light filtering properties. Panel 6 combines guaiazulene with astaxanthin, demonstrating the potential for enhanced broad-spectrum protection. Panel 7 displays a sunscreen formulated with astaxanthin, highlighting its distinct color and potential benefits.

3.1.2 Particle Size Analysis of Astaxanthin Sunscreen

The astaxanthin-based sunscreen exhibits a golden-orange translucent hue. Upon microscopic examination, it was observed that the sunscreen contains uniformly distributed small particles, as depicted in Figure 2. This uniform particle distribution is indicative of a homogeneous formulation, which is essential for consistent application and effectiveness of the sunscreen.

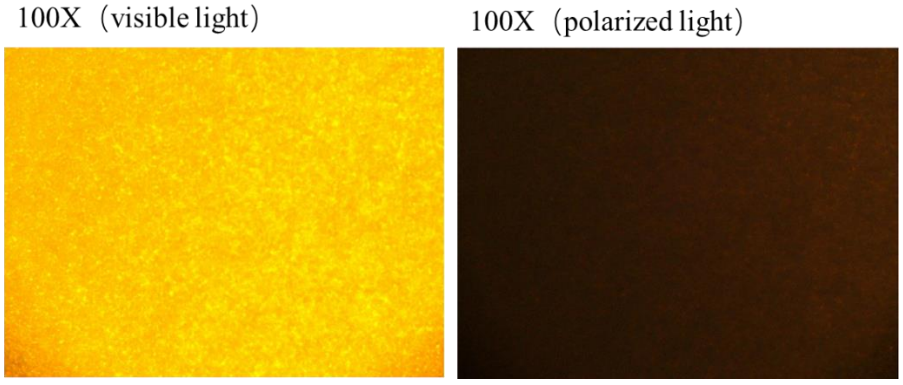

Figure 2. The colour and particles of astaxanthin sunscreen at 100X magnification

Our analysis of particle size distribution demonstrated a significant correlation between the differentiation rate (Diff%, D) and particle size, as detailed in Table 2. The results of the astaxanthin sunscreen particle size analysis (Figure 3) indicated a unimodal distribution with a

sharp peak, where 57.77% of particles fall within the 0.200-0.500 µm range, 10.70% within the 0.500-1.000 µm range, 6.40% within the 0.100-0.200 µm range, and the remaining particles are larger than 1.00 µm. The average volume diameter of the particles was calculated at 2.521 µm, while the average surface diameter was 0.401 µm. The average particle number's diameter was 0.242 µm. The surface area was determined to be 5549 m²/kg, with an unexplained residual (error) of 1.939%, and a light shading percentage of 8.76%.

These findings suggest that the astaxanthin sunscreen is uniformly emulsified and exhibits excellent dispersibility in water, maintaining high transmittance. This uniform particle size distribution is crucial for ensuring consistent application and efficacy of the sunscreen.

Table 2. The correlation between differentiation rate (Diff%, D) and particle size.

D03 = 0.176 µm	D06 = 0.197 µm	D10 = 0.176 µm	D16 = 0.244 µm	D25 = 0.275 µm
D50 = 0.377 µm	D75 = 1.013 µm	D84 = 4.663 µm	D90 = 9.778 µm	D97 = 18.17 µm

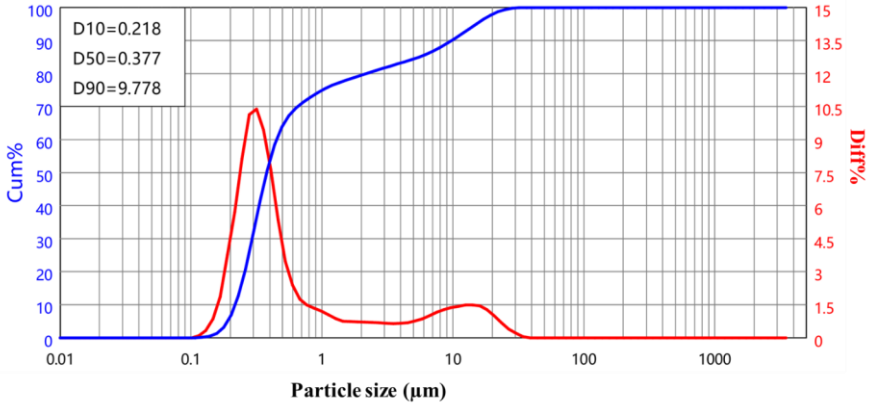

Particle size (µm)	Percentage
0.000-0.050	0.00%
0.050-0.100	0.00%
0.100-0.200	6.40%
0.200-0.500	57.77%
0.500-1.000	10.70%
1.000-2.000	4.65%
2.000-5.000	4.85%
5.000-10.000	5.86%
10.00-20.00	7.68%
20.00-45.00	2.07%

Figure 3. The particle size distribution of astaxanthin sunscreen. Left: particle size distribution. Right: Percentage of differrent particle size. Cum%: cummulative percentage. Diff%: differential particle size distribution.

3.2 Astaxanthin Sunscreen is Milk and Non-irritating

The astaxanthin-containing sunscreen was subjected to a human patch test to assess its safety and tolerance. The results demonstrated that none of the volunteers experienced any adverse reactions to either of the two test samples, suggesting that the sunscreens are mild and non-irritating when applied to general human skin. This finding is crucial as it indicates the potential for these sunscreens to be used safely in daily skincare routines without causing skin irritation or discomfort.

3.3 Enhancement of SPF Value by Astaxanthin

3.3.1 *In Vitro* Enhancement of SPF Value

The machine measurement results are summarized in Table 4. The SPF of the reference sample was determined to be 16.75 ± 0.34. The theoretical SPF value of the reference sample was calculated to be between 13.7 and 18.50. The SPF values for the sunscreen and astaxanthin sunscreen were measured at 104.72 ± 0.63 and 131.0 ± 0.3, respectively. This

indicates that the incorporation of astaxanthin into the formula significantly enhanced the UVB protection efficacy by 25.14% ($p < 0.001$).

Table 4. The *in vitro* measured SPF value.

Sample	SPF (Mean ± SEM)	Change rate
Reference sample	16.75 ± 0.34	/
Sunscreen	104.72 ± 0.63	9.03%
Astaxanthin sunscreen	131.0 ± 0.33	$p = 0.048$

3.3.2 *In Vivo* Enhancement of SPF Value Without Affecting PFA Value

The *in vivo* clinical SPF and PFA value test results are detailed in Table 5. The SPF of the reference sample was found to be 15.2 ± 0.3, while the SPF values for the sunscreen and astaxanthin sunscreen were 43.2 ± 3 and 47.1 ± 4.8, respectively, representing a 9.03% (p = 0.048) increase in sun protection efficacy. These results further substantiate the enhancing effect of astaxanthin on sun protection efficacy.

The PFA of the reference sample was measured at 4.4 ± 0.0. The PFA values for the sunscreen and astaxanthin sunscreen were 16.2 ± 2.8 and 16.0 ± 0.3, respectively. This indicates that astaxanthin did not impact the UVA protection efficacy of the formula.

Table 5 - The *in vivo* clinical test measured SPF and PFA values.

Sample	SPF (Mean ± SEM)	PFA (Mean ± SEM)
Reference sample	15.2 ± 0.3	4.4 ± 0
Sunscreen	43.2 ± 3	16.2 ± 2.8
Astaxanthin sunscreen	47.1 ± 4.8	16.0 ± 1.3

3.3.5 Rutin Showed Excellent *In Vitro* Blue Light Absorption

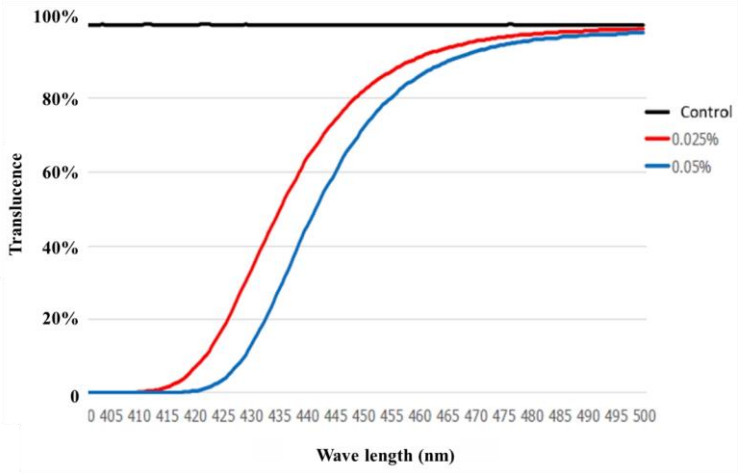

Figure 4. The blue light absorption of rutin solution.

The results of the *in vitro* blue light absorption test are depicted in Figure 4. The findings revealed that a 0.5% rutin solution of the reference sample exhibited an SPF value of 15.2 ± 0.3. In contrast, the SPF values for the sunscreen and astaxanthin sunscreen were determined to be 43.2 ± 3 and 47.1 ± 4.8, respectively. This indicates a significant enhancement in sun protection efficacy of 9.03% ($p = 0.048$) when astaxanthin is incorporated into the sunscreen formulation. These results further substantiate the potential of astaxanthin to augment the sun protection capabilities of sunscreens.

3.4 Astaxanthin Sunscreen Demonstrated Very Low Skin Penetration Activity

The Raman spectroscopy analysis identified the characteristic Raman peaks of astaxanthin sunscreen at 959 cm^{-1}, 1092 cm^{-1}, 1198 cm^{-1}, 1263 cm^{-1}, 1410 cm^{-1}, 1448 cm^{-1}, 1519 cm^{-1}, I558 cm^{-1}, 1612 cm^{-1}, 2904 cm^{-1}, 29614 cm^{-1} and 3076 cm^{-1} (Figure 5A).

In-depth analysis of the Raman images revealed the content distribution map at different skin depths (Figure 5B). After 6 hours of application, the astaxanthin sunscreen penetrated only into the surface of the stratum corneum and did not reach the epidermis or dermis layers. This indicates that the oil-in-water-in-oil sunscreen formulation technology effectively prevents significant penetration of the sunscreen into the skin.

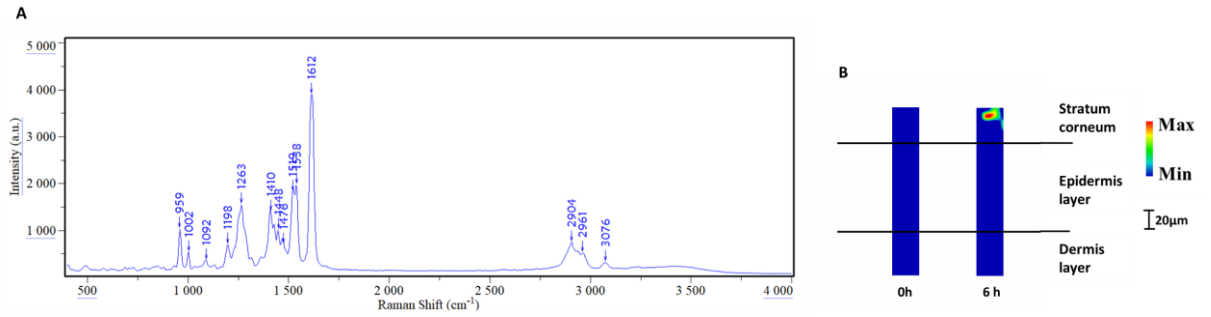

Figure 5. The Raman spectroscopy analysis found very low skin penetration for astaxanthin sunscreen. A: Raman spectrogram of astaxanthin sunscreen. B: Astaxanthin sunscreen content distribution map at different depths of the skin.

3.5 Astaxanthin Sunscreen Provided Good Anti-pollution Efficacy

The results of the anti-pollution experiment (Figure 5) show that the back of the left hand, which was treated with astaxanthin sunscreen, exhibited almost no visible black carbon powder residue. In contrast, the back of the right hand, which served as the control, displayed a significant amount of black carbon residue. This indicates that the sunscreen effectively formed a protective film on the skin, preventing pollutants from coming into contact with it.

Figure 6. Astaxanthin sunscreen provided good anti-pollution efficacy to the skin.

3.6 Astaxanthin Sunscreen Provided Freshing and Non-sticky Sensory Experience

The results (Figure 5) indicate that only 2–4 foam balls adhered to the back of the left hand after treatment with astaxanthin sunscreen. This demonstrates that the sunscreen provided a refreshing and non-sticky sensory experience on the skin.

Figure 7. Astaxanthin sunscreen provided freshing and non-sticky sensory experience.

4. Discussion

This study presents a novel sunscreen formulation technology that integrates a water-in-oil system using silicone oil to encapsulate UV absorbers and an oil-in-water system containing a water-based solution with PPG-13-decyl-tetradecet-24 and polyquaternium-61 to encapsulate active ingredients such as astaxanthin and rutin, resulting in a translucent oil-in-water-in-oil system. Visual examination indicated that the addition of colored active ingredients imparted a range of aesthetically pleasing colors to the sunscreen. Specifically, rutin added a greenish tint, astaxanthin produced an orange hue, and their combination yielded a blue color, which is attributable to rutin's absorption of blue light. Microscopic observation revealed that the astaxanthin sunscreen exhibited a golden-orange translucent color with uniformly distributed particles, primarily ranging from 200 to 500 nm in size. Further in vitro and in vivo SPF analysis demonstrated that the incorporation of astaxanthin significantly enhanced SPF values. In vitro blue light absorption tests showed that a 0.5% rutin solution could block over 90% of blue light below 430 nm and approximately 50% below 445 nm. The inclusion of rutin in sunscreen formulations can extend protection to blue light, addressing a growing market demand.

Additionally, *in vivo* testing demonstrated the sunscreen's effectiveness in preventing particulate matter from adhering to the skin after rinsing with tap water.

5. Conclusion

In conclusion, this innovative sunscreen formulation technology offers broad-spectrum protection against UV and blue light, incorporates non-penetrating filters, provides air pollution defense, features customizable jelly textures with vibrant color options, and delivers skin tone correction benefits. This technology renders sunscreen products multifunctional, more effective, and much more enjoyable.

References

[1] Aguilera J, Gracia-Cazaña T, Gilaberte Y. New developments in sunscreens. *Photochem Photobiol Sci.* 2023; 22(10): 2473-2482.

[2] Matta MK, Florian J, Zusterzeel R, et al. Effect of sunscreen application on plasma concentration of sunscreen active ingredients: a randomized clinical trial. *JAMA.* 2020; 323(3): 256–267.

[3] Romanhole RC, Fava ALM, Tundisi LL, et al. Unplanned absorption of sunscreen ingredients: Impact of formulation and evaluation methods. *Int J Pharm.* 2020; 591: 120013.

[4] Olejnik A, Goscianska J. Incorporation of UV absorbers into oil-in-water emulsions—release and permeability characteristics. *Appl Sci.* 2023; 13: 7674.

[5] Hamadeh A, Nash JF, Bialk H, Styczynski P, Troutman J, Edginton A. Mechanistic skin modeling of plasma concentrations of sunscreen active ingredients following facial application. *J Pharmac Sci.* 2024; 113: 806-825.

[6] Heneweer M, Muusse M, Van Den Berg M, Sanderson JT. Additive estrogenic effects of mixtures of frequently used UV absorbers on pS2-gene transcription in MCF-7 cells. *Toxicol Appl Pharmacol.* 2005; 208: 170–177.

[7] Schlumpf M, Cotton B, Conscience M, et al. *In vitro* and *in vivo* estrogenicity of UV screens. *Environ Health Perspect.* 2002; 109: 239–244.

[8] Safety and Technical Standards for Cosmetics. National Medical Products Administration. GGTG-2015-13053. 2015, 268.

[9] GB/T 40219-2021. General specification for Raman spectrometers. ICS 71.040.10. 2021.